NEW MODELS OF ENDOGENIC HEAT FROM ENCELADUS' SOUTH POLAR FRACTURES. O. Abramov[1] and J. R. Spencer[2], [1]U.S. Geological Survey, Astrogeology Science Center, 2255 N. Gemini Dr., Flagstaff, AZ 86001 (*oabramov@usgs.gov*), [2]Southwest Research Institute, 1050 Walnut St., Suite 300, Boulder, CO 80302.

Introduction: The south polar region of Enceladus, a small icy satellite of Saturn, consists of young, tectonically deformed terrain dominated by four roughly parallel, ~2-km wide linear depressions dubbed "tiger stripes" [e.g., 1]. Observations by multiple instruments on the Cassini spacecraft describe anomalously high heat fluxes associated with these tiger stripes [e.g., 2], along with active plumes of water vapor and ice particles that originate from them [e.g., 3]. Several explanations for the observed elevated temperatures and the resulting plume have been proposed, including venting from a subsurface reservoir of liquid water [e.g., 1], sublimation of surface ice [e.g., 2], decompression and dissociation of clathrates [e.g., 4], and shear heating [e.g., 5]. These mechanisms predict a range of vent temperatures: ~140 K for clathrate decompression [4], >180 K for sublimation of H_2O [2], and up to 273 K for the shallow reservoir of liquid water [1]. In addition, constraining the width of the crack may further elucidate the mechanism: subsurface ice melting is likely unless the crack width is greater than ~10 cm [6].

The present work builds on the foundation established by [7], which sought to elucidate the underlying physical mechanism by constraining vent temperatures and widths, using a model in which the observed thermal signature results primarily from conductive heating of the surface by warm subsurface fractures. The present work involves: (i) making improvements to the model, as outlined below, and (ii) applying the model to new Cassini Composite InfraRed Spectrometer (CIRS) tiger stripe spectra, which represents up to an order of magnitude improvement in spatial resolution over the data sets used in [7], as well as a greatly improved signal-to-noise ratio.

Methods: The basic steady-state thermal model that forms the basis of this work was published in [7], and included two free parameters: fracture temperature and fracture width. The parameters of the new model include (i) the temperature of the vent, (ii) the number of vents within a tiger stripe – multiple parallel fractures have been observed in high spectral resolution ISS images to lie within regions of the plume sources, (iii) the width of each individual vent, and (iv) geometry of the surface. In addition, dynamic model resolution has been implemented. The new model rapidly explores parameter space by automatically generating temperature distributions in and around tiger stripes based on specified constraints, acquiring synthetic CIRS spectra of the model surfaces, and comparing them to CIRS observations using statistical methods.

Temperature distributions around tiger stripes on Enceladus are modeled in two dimensions using HEATING 7.3, a multidimensional, finite-difference heat conduction code developed at Oak Ridge National Laboratory [8]. The model includes heat transfer by conduction in the subsurface from a vertical fracture held at constant temperature, and by radiation at the surface. Cassini ISS [e.g., 1] and VIMS observations [e.g., 9], as well as thermal modeling [7], suggest coarse-grained crystalline water ice near the tiger stripes, perhaps due to sintering of surface grains by vapor condensed from the plumes. The HEATING library provides temperature-dependent thermophysical parameters appropriate for this material over the full range of temperatures in the model. Emissivity of fresh water ice ranges from ~0.94 to over 0.99 at the wavelengths of interest, and is incorporated into the model. The bottom and right boundaries are insulating, and heat is lost by radiation through the upper boundary, which is radiatively heated to an equilibrium temperature constrained by Cassini CIRS.

Results: A preliminary model incorporating multiple fractures was put together, and a chi-square statistic was used to compare the synthetic spectrum to a single CIRS spectrum: a combined FP3/FP4 observation of Damascus Sulcus, acquired during the August 2010 flyby. The automated parameter exploration, including the number of fractures, fracture temperature, and fracture width, was mapped in chi-squared space (**Fig. 1**) to visualize trends. Temperatures of the vents were varied from 170 K to 273 K in increments of 1 K; number of vents was varied from 1 to 6; and vent widths were varied from 0 to 20 m in increments of 1 cm. The best model match to data occurred at four 19-m fractures, each at 185 K. This moderate temperature does not necessitate invoking near-surface liquid water. This result is also in good agreement with a temperature of 197 ± 20 K and a width of 9 m derived from an April 2012 VIMS observation of Baghdad Sulcus [10].

The comparison of the synthetic spectrum produced by this combination of parameters and the actual CIRS FP3/FP4 spectrum of Damascus tiger stripe is shown in **Fig. 2**. The excellent agreement between the model and the data, combined with Cassini ISS observations suggestive of multiple fractures in this region, validate the model and pave the way to further applications of this model to PDS-archived CIRS data.

Acknowledgements: This work was funded by the NASA Cassini Data Analysis Program (CDAP) under award number NNH13AV61I.

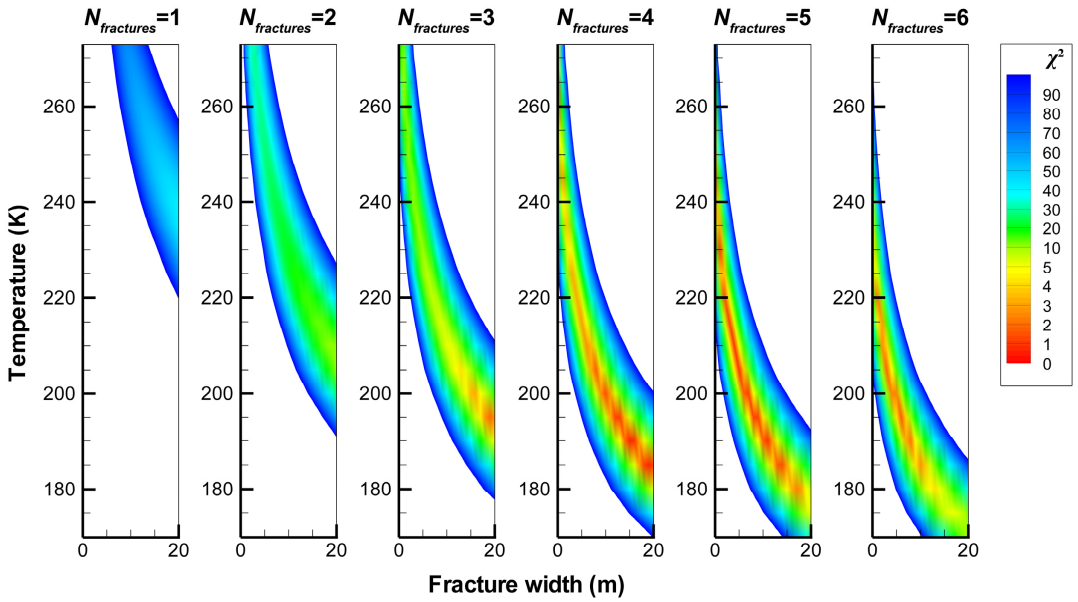

Fig. 1. Automated exploration of parameters in chi-squared space. CIRS data is the combined FP3/FP4 observation of the Damascus tiger stripe at 0.8 km/pixel, obtained during the August 2010 flyby. Three parameters are varied: fracture temperature, fracture width, and number of fractures.

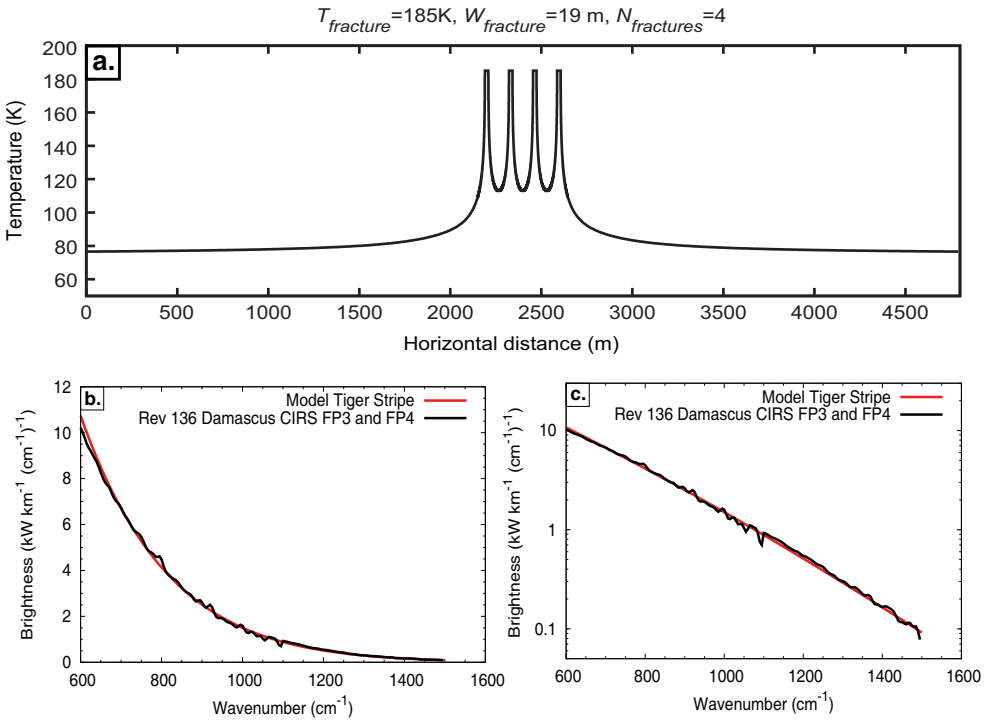

Fig. 2. Best model match to the CIRS FP3/FP4 spectrum of Damascus tiger stripe, obtained during the August 2010 flyby. CIRS footprint is 800 m, centered on the fractures. (a) Model surface temperature distribution. (b) Comparison between model and CIRS data. (c) Comparison between model and CIRS data on a log scale.

References: [1] Porco C.C. et al. (2006) *Science*, 311, 1393-1401. [2] Spencer J.R. et al. (2006) *Science*, 311, 1401-1405. [3] Hansen C.J. et al. (2006) *Science*, 311, 1422-1425. [4] Kieffer S.W. et al. (2006) *Science*, 314, 1764-1766. [5] Nimmo F. et al. (2007) *Nature*, 447, 289-291. [6] Ingersoll A. and A. Pankine (2010) *Icarus*, 206, 594-607. [7] Abramov O. and J.R. Spencer (2009) *Icarus*, 199, 189-196. [8] Childs K.W. (1993) ORNL/TM-12262, Oak Ridge National Laboratory. [9] Brown R.H. et al. (2006) *Science*, 311, 1425-1428. [10] Goguen J. D. et al. (2013) *Icarus*, 226, 1128-1137.